[Frontiers in Bioscience 14, 1939-1944, January 1, 2009]

In vivo microCT quantification of lung tumor growth in SPC-raf transgenic mice

Thomas Rodt[1,2], Christian von Falck[1,2], Roman Halter[2], Kristina Ringe[1], Hoen-Oh Shin[1], Michael Galanski[1], Juergen Borlak[2]

[1]Department of Diagnostic Radiology, Hannover Medical School, Hannover, Germany, [2]Dept. of Pharmaceutical Research und Medical Biotechnology, Fraunhofer-Institute for Toxicology and Experimental Medicine, Hannover, Germany

TABLE OF CONTENTS

1. ABSTRACT

Lung cancer is the most common cancer worldwide. Early detection might reduce morbidity. In this study we evaluate a microCT imaging algorithm to assess *in-vivo* tumour load and quantification of tumour growth in a transgenic disease model of lung adenocarcinomas. MicroCT was carried out with n=10 SPC-raf transgenic mice without gating in spontaneously breathing and isoflurane anaesthetised animals. Segmentation of the air-filled spaces was obtained using a region growing algorithm by 3 independent observers. Inter- and intra-observer variability of the algorithm was determined and compared against an alternative region growing algorithm. Due to the multiple very small tumor nodules that occur and the low signal-to-noise ratio direct volumetric measurement of solitary tumor nodules is not feasible. However, tumor growth can be assessed by measuring the decrease in the segmented volume of the aerated lung areas. The presented algorithm can thus be used to evaluate therapeutic efficacies of novel treatment strategies. The imaging algorithm allows *in vivo* quantification of lung tumor load and tumor growth in transgenic mice with an acceptable intra- and interobserver variability.

2. INTRODUCTION

Lung cancer is the most common cancer worldwide and tobacco smoking is considered to be the major risk factor accounting for nearly 90% of all cases. To better understand the molecular causes of this disease a number of genetic disease models have been developed. In the past a disease model was described where overexpression of the serine-threonine-kinase c-raf to alveolar epithelium was achieved by use of the surfactant protein C (SPC) promoter. Essentially targeted overexpression of c-raf to lung epithelium resulted in adenocarcinomas of the lung, with multifocal adenomatous hyperplasia being defined as the earliest proliferative lesion of dysplastic cells (1-3). The transgenic animal model described here allows to probe for mechanisms of carcinogenesis based on the ras-raf mitogen activated cascade, that plays a crucial role in the development of adenocarcinomas of the lungs.

Furthermore, this genetic disease model offers the unique opportunity to study carcinogenesis in more realistic setting as compared to models of implanted (xenograft) tumours into immunodeficient mice. In fact, the

animals are still immunologically competent, whilst the continuous expression of the transgene secures continuous tumor pressure. Hitherto, the relevance of overexpressed protooncogenes or disabled tumor suppressor genes can be studied (1, 4, 5). Additionally these animal models are invaluable to investigate mode of action and efficacy of novel therapeutics.

In this regard validated *in-vivo* imaging of the tumor load and quantification of tumor growth would be extremely beneficial as this would help to evaluate novel treatment strategies. Importantly, these techniques could help to reduce the number of laboratory animals needed to study certain pathologies, as longitudinal data collection in an individual animal becomes feasible.
Different imaging modalities have been described and their advantages and disadvantages have been discussed for small animal imaging (6). MicroCT allows comparatively fast assessment of morphology (7). Furthermore metabolic imaging by microPET or optical imaging of the examined tissue can be added (8, 9). The correlation with morphology, e.g. by microCT / microPET registration, enables exact localization of this metabolic information. More recently, molecular imaging of new drugs at the tumor site or imaging of disease candidate genes has become feasible (10).

Due to the nature of the detectors used in volume computed tomography, microCT has limitations in soft-tissue differentiation due to the low-signal-to-noise-ratio and low contrast resolution (6). As reported herein the SPC-raf transgenic mouse model developed disseminated adenocarcinomas; due to the multiple very small tumor nodules that occur a direct volumetric measurement of a single lesion is not feasible. There is a need to develop a quantification algorithm for microCT taking the multifocal and diffuse tumor growth into account.

Here we report a novel microCT imaging algorithm for assessment of lung tumor burden and quantification of tumor growth in SPC-raf transgenic mice.

3. MATERIALS AND METHODS

3.1. Animals

The SPC-raf transgenic mouse strain has already been described in detail (3). In the transgenic animal model, the first morphological changes occur in distinct areas of the lung such as subpleural areas in the first weeks to months. The sequential development of multifocal atypical adenomatous hyperplasia, which can be defined as the initial proliferative lesion of dysplastic epithelium, and thereafter adenocarcinoma of the lung are observed. At the age of 8 months, 60-70% of the lung show tumor (1) (Figure 1). Transgenic mice were maintained as hemizygotes in the C57BL/6 mouse strain background. Animals were housed in polycarbonate cages. Absorbent softwood was used as bedding material. Food and water was given ad libitum. The temperature and relative humidity of the animal room was kept constant and recorded continuously. When the animals started to show signs of illness or grew to old they were euthanized.

3.2. Imaging

10 microCT (GE Explore Locus) examinations were carried out without gating. Imaging was performed with anaesthetized animals placed in prone position on a multimodality bed that allows changes between imaging modalities, which were used for other studies, without repositioning of the animal. Isoflurane inhalation anesthesia was administered using a nose cone. Respiratory monitoring was performed using a pressure transducer pad that was placed under the animal´s chest (Figure 2). MicroCT was performed with 80 kV tube voltage and 450 µA tube current. No contrast media was administered. Reconstruction voxel size was 0.094 x 0.094 x 0.094 mm, the FOV (field of view) was adapted to the size of the chest (Figure 3). The scanning time was 17 minutes.

3.3. Post-processing

Data-analysis of the microCT-data was performed using the software MevisLab (Mevis Research, Bremen, Germany) (11, 12). Direct measurement of tumor growth was not feasible due to the multifocal tumor nodules and diffuse tumor growth. However, the reduction of air-filled spaces of the lungs correlates with tumor growth and thus was used for quantification. A region-growing segmentation algorithm (algorithm1) was applied. Segmentation was carried out using 20-40 seed points, the segmentation threshold tolerance of the region growing algorithm was set to 2 % (Figure 4). The seed points were randomly placed in the aerated lung areas. Intra- and interrater-variability of the segmentation of the air-filled spaces was assessed in 10 animals that were segmented 3 times by 3 observers. Segmentation was performed 3 times in a row. The raters worked completely independent and were not informed about the results of the other raters. The inter- / intraobserver variability of this algorithm were compared against the values of a second region growing algorithm (algorithm2), where nonlinear diffusion filtering was performed with regard to the low signal-to-noise ratio of the datasets. The segmentation threshold tolerance was set to 3%. All other parameters were identical to algorithm1. For the comparison segmentation was carried out by two raters.

3.4. Histopathological correlation / necropsies

The histopathology of lung cancer was described earlier, showing the development of disseminated atypical adenomatous hyperplasia leading to adenocarcinomas of the lung (1, 3). Necropsies were performed when the animals had to be sacrificed due to clinical condition. In 7 animals necropsies were performed immediately, in 3 animals necropsies were performed at a later point in time. In these 3 cases follow up examinations were performed.

3.5. Statistical analysis

Intra-observer variabilities were calculated for each observer on the basis of the variances of three independent measurements, performed in all of 10 animals: the square root of the mean of the 10 variances was divided by the mean of the observations, and was expressed as percentage. Similar, the variance between the three observers of the mean measurements per animal was used to calculate the inter-observer variability. Analysis of the

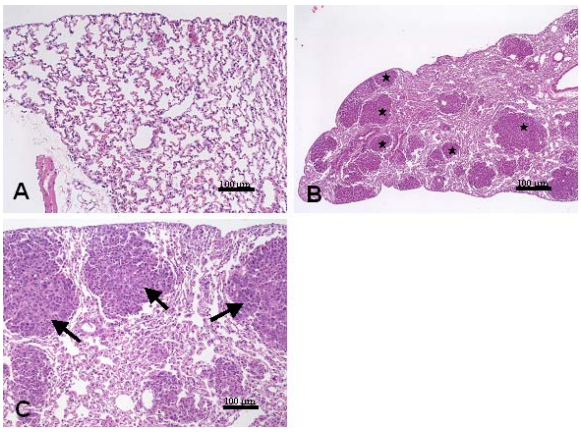

Figure 1. Histopathology of the lung of SPC-raf transgenic mice. A: normal lung; B: lung of a transgenic mouse with multifocal atypical adenomatous hyperplasias, leading to adenocarcinoma of the lung (asterisks). C: higher magnification showing the lung tumors in more detail (arrows).

Figure 2. A: Multimodality bed with nose cone and respiratory monitoring pad. B: Mouse positioned for scanning in prone position under inhalation anaesthesia.

inter- / intraobserver variability of the described region growing algorithm1 against algorithm2, where nonlinear diffusion filtering was performed and the threshold tolerance was increased, was carried out using a 2-factorial analysis of variance.

4. RESULTS

4.1. Imaging

The inhalation anesthesia was well tolerated. The recovery time to gain full motor agility after the anesthesia was about 5 minutes. No adverse effects were observed due to the handling and imaging of the animals. The microCT images provided sufficient anatomical detail to assess the lungs. As the respiratory rate was comparatively high (respiratory rate approximately 80-100/min), artifacts due to respiratory chest wall movements were acceptable. It was observed, that the artifacts increased with decreasing respiratory rate and were more severe in the inferior parts of the lungs. Due to the low signal-to-noise ratio direct measurement of singular nodules was not feasible. The diffuse and multifocal lung tumor could be imaged to sufficient detail. In later stages of the disease consolidated lung areas were seen. As the animal model had showed no significant occurrence of atelectasis or pneumonia when it was validated by histopathology, these were interpreted as confluence-tumors.

4.2. Post-processing

Placement of the seed-points was unproblematic in all cases. The post-processing time using region growing algorithm1 was approximately 2 minutes, using region growing algorithm2 the time increased to approximately 10 minutes, mainly due to the filtering prior to the actual segmentation. Spread of the segmented volume into adjacent structures occurred in two cases using algorithm2. Apart form this, the algorithms were robust. The obtained segmentation data could be further post-processed using the software, e.g. three-dimensional images of the segmented lung volume could be generated. The measured volumes were in the approximated range of 0,2 to 0,5 ml.

4.3. Histopathological correlation / necropsies

Macroscopic assessment of the external aspect of the lungs at necropsy correlated to imaging findings in all cases.

4.4. Statistical analysis

Intra-observer variability was 3.74 %, 6.06 % and 5.61 % for observer 1, 2 and 3 using algorithm1 respectively. Overall intra-observer variability for algorithm1 was 5.14 %. Inter-observer variability for the mean values of the three measurements by each observer was 6.54 %. Analysis of the inter- / intraobserver variability of the described region growing algorithm1 against algorithm2 using a 2-factorial analysis of variance, did not show significantly different variability values. In fact algorithm2 achieved slightly worse variability values.

5. DISCUSSION

The SPC-raf transgenic mouse model provides excellent conditions to study the development, disease progression, and treatment of lung adenocarcinoma (1, 3). Imaging of the tumor provides evidence for progression or regression of the disease without killing the animal. This is extremely helpful to further characterize the pathogenesis of lung cancer and to evaluate efficacies of new treatment strategies. We therefore aimed at developing an imaging algorithm to assess tumor load and growth pattern. Such an algorithm can enable longitudinal as well as treatment response studies in a more realistic manner.

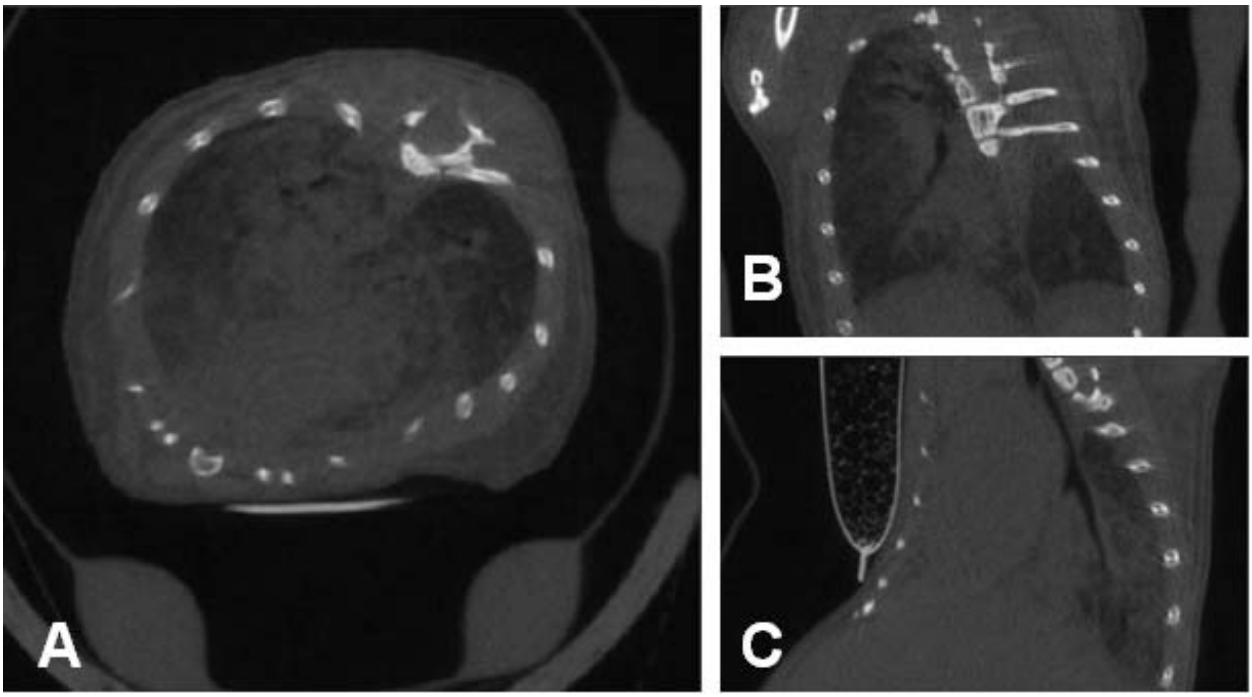

Figure 3. A: Axial microCT of a SPC-raf transgenic mouse. Diffuse micronodular opacities representing the tumors. B: Coronal image C: Sagital image.

The diffuse tumor growth pattern in SPC-raf transgenic mice impairs direct 1-dimensional or volumetric measurements of a single lesion. This problem has also been described for image analysis of bronchioloalveolar carcinoma in humans (14, 15). The animal model studied here has been comprehensively analyzed by histopathology. As the animals are immuno-compentent, there is no evidence of infectious consolidation or atelectasis. Therefore, the measurement of the aerated lung volume can be used as an inverse surrogate for tumor burden and growth.

This study demonstrates that the measurement of the aerated lung volume is technically feasible with an acceptable inter- and intra-observer variability using algorithm1. Algorithm2 yielded slightly worse results as compared with algorithm1. The theoretical approach of the algorithm2 was to reduce noise by diffusion filtering allowing a more precise volume quantification taking advantage of the increased signal-to-noise ratio. This may lead to a more precise measurement, and may also allow the use of a smaller threshold tolerance value, again with beneficial effects on the precision of the measurement. Simultaneously, the risk of an incorrect spread of the segmentation volume into adjacent normal structures would be decreased. However, algorithm2 did not provide better results. As it was shown the threshold tolerance value could not be decreased without spread of the segmentation volume into adjacent structures, which occurred in two cases. Furthermore, the segmentation time increased considerably due to the filtering process. In conclusion the diffusion filtering used did not provide beneficial results in this case.

In this study data was acquired without respiratory gating. Therefore an average of the lung volume over time was assessed. The proposed beneficial effect of respiratory gating on the image quality and potentially on the precision of the measurement of the aerated lung volume could lead to a further refinement of the estimate of the tumor growth if gating was applied (6). Respiratory gating would allow assessment of lung volume at a certain phase of the respiratory cycle. However, as respiratory gating increases the data-acquisition time changes in the respiratory rate might increase due to longer anesthesia if the animals are not intubated. A changed respiratory rate might consequently lead to changes of the tidal volume. Furthermore, even with respiratory gating it is difficult to generate images at the inspiration maximum without motion artefacts as this phase is very short and variable in not intubated animals, as opposed to intubated animals where a plateau can be artificially created at the inspiration maximum. As the volumetric measurements of the aerated lung areas were not compared against a second technique, e.g. a volumetric analysis of histopathological sections, the absolute values are not validated as yet. The primary goal of this study was to demonstrate the robustness of the developed post-processing algorithm for this specific purpose. Correlation to histopathological sections would provide the challenge to secure a defined filling pressure of the lung fixating agent and to quantify the aerated volume using the section cuts. Correlation of the results to pulmonary function testing was also considered. However, assessment of the total ventilated volume is complex and the tidal volume which is easier to measure would not necessarily correlate to the total ventilated volume. Measurements of defined water volumes using algorithm1,

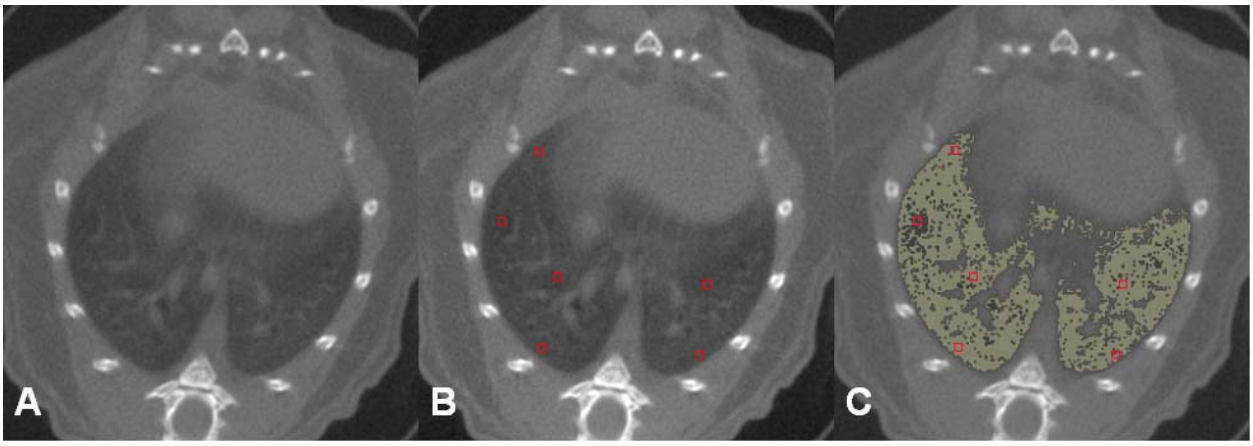

Figure 4. Segmentation of the air-filled spaces. A: Axial microCT. B: Placement of seed points, a position in bronchi or vessels is avoided. C: Segmentation result using region growing algorithm1.

prior to the presented study, yielded precise results. However, we expect the measured volumes to underestimate the aerated lung volume. This is mainly due to the fact, that the algorithms was tailored to prevent the segmentation volume from spreading into spaces adjacent to the aerated lung volumes. Nonetheless, the volumetric values can be used to assess relative increase or decrease if a baseline has been acquired for comparison. The tumor load without a baseline exam can not be assessed quantitatively. Nonetheless the volumetric measurement even without a baseline exam for comparison allows a more precise assessment compared to the purely visual analysis of the diffuse and multifocal tumor pattern.

In the future, we will study the correlation of aerated lung volume to individual characteristics such as age, weight, and gender in addition to the tumor burden both inter- and intraindividually. This could enable us to generate time curves of the tumor models, allowing to assess the tumor load at a specific age in comparison to the average tumor load.

In conclusion the presented algorithm allowed quantification of the aerated lung volume as a surrogate measure for tumor load with acceptable inter- and intra-observer variability.

6. ACKNOWLEDGMENT

We would like to thank Hartmut Hecker and Jana Prokein for their support concerning the statistical analysis. The financial support of a research grant from GE Healthcare is gratefully acknowledged.

7. REFERENCES

1. Ruetters H, P. Zuerbig, R. Halter, J. Borlak: Towards a lung adenocarcinoma proteome map: studies with SP-C/c-raf transgenic mice. *Proteomics* 6, 3127-3137 (2006)

2. Nomori H, T. Ohtsuka, T. Naruke, K. Suemasu: Differentiating between atypical adenomatous hyperplasia and bronchioloalveolar carcinoma using the computed tomography number histogram. *Ann Thorac Surg* 76, 867-871 (2003)

3. Kerkhoff E, L.M. Fedorov, R. Siefken, A.O. Walter, T. Papandopoulos, U.R. Rapp: Lung-targeted expression of the c-raf-1 kinase in transgenic mice exposes a novel oncogenic character of the wild-type protein. *Cell Growth Differ* 11, 185-190 (2000)

4. Ehrhardt A, T. Bartels, A. Geick, R. Klocke, D. Paul, R. Halter: Development of pulmonary bronchiolo-alveolar adenocarcinomas in transgenic mice overexpressing murine c-myc and epidermal growth factor in alveolar type II pneumocytes. *Br J Cancer* 84, 813-818 (2001)

5. Ehrhardt A, T. Bartels, R. Klocke, D. Paul, R. Halter: Increased susceptibility to the tobacco carcinogen 4-(methylnitrosamino)-1-(3-pyridyl)-1-butanone in transgenic mice overexpressing c-myc and epidermal growth factor in alveolar type II cells. *J Cancer Res Clin Oncol* 129, 71-75 (2003)

6. Bartling S, W. Stiller, W. Semmler, F. Kiessling: Small Animal Computed Tomography Imaging. *Current Medical Imaging Review*s 3, 45-59 (2007)

7. Kennel SJ, I.A. Davis, J. Branning, H. Pan, G.W. Kabalka, M.J. Paulus: High resolution computed tomography and MRI for monitoring lung tumor growth in mice undergoing radioimmunotherapy: correlation with histology. *Med Phys* 27, 1101-1107 (2000)

8. Chang CH, H.E. Wang, S.Y. Wu, K.H. Fan, T.H. Tsai, T.W. Lee, S.R. Chang, R.S. Liu, C.F. Chen, C.H. Chen, Y.K. Fu: Comparative evaluation of FET and FDG for differentiating lung carcinoma from inflammation in mice. *Anticancer Res* 26, 917-925 (2006)

9. Chang CH, M.L. Jan, K.H. Fan, H.E. Wang, T.H. Tsai, C.F. Chen, Y.K. Fu, T.W. Lee: Longitudinal evaluation of tumor metastasis by an FDG-

microPet/microCT dual-imaging modality in a lung carcinoma-bearing mouse model. *Anticancer Res* 26, 159-166 (2006)

10. Grimm J, D.G. Kirsch, S.D. Windsor, C.F. Kim, P.M. Santiago, V. Ntziachristos, T. Jacks, R. Weissleder: Use of gene expression profiling to direct *in vivo* molecular imaging of lung cancer. *Proc Natl Acad Sci USA* 102, 14404-14409 (2005)

11. Bitter I, R. Van Uitert, I. Wolf, L. Ibanez, J.M. Kuhnigk: Comparison of four freely available frameworks for image processing and visualization that use ITK. *IEEE Trans Vis Comput Graph* 13, 483-493 (2007)

12. Heussel CP, T. Achenbach, C. Buschsieweke, J. Kuhnigk, O. Weinheimer, G. Hammer, C. Düber, H.U. Kauczor: [Quantification of pulmonary emphysema in multislice-CT using different software tools] *Rofo* 178, 987-998 (2006)

13. Parodi RC, F. Sardanelli, P. Renzetti, E. Rosso, C. Losacco, A. Ferrari, F. Levrero, A. Pilot, M. Inglese, G.L. Mancardi: Growing Region Segmentation Software (GRES) for quantitative magnetic resonance imaging of multiple sclerosis: intra- and inter-observer agreement variability: a comparison with manual contouring method. *Eur Radiol* 12, 866-871 (2002)

14. Lau D, A. Seibert, D. Gandara, L. Laptalo, E. Geraghty, C. Coulon: Computer-assisted image analysis of bronchioloalveolar carcinoma. *Clin Lung Cancer* 6, 281-286 (2005)

15. Nagao M, K. Murase, Y. Yasuhara, J. Ikezoe, K. Eguchi, H. Mogami, K. Mandai, M. Nakata, Y. Ooshiro: Measurement of localized ground-glass attenuation on thin-section computed tomography images: correlation with the progression of bronchioloalveolar carcinoma of the lung. *Invest Radiol* 37, 692-697 (2002)

Abbreviations: c-raf: (rapidly growing fibrosarcoma) a proteinkinase; SPC: surfactant protein C; ras: (rat sarcoma) oncogen; CT: computed tomography; PET: positron emission tomography

Key Words: MicroCT, Small animal imaging, Transgenic animal model, Lung tumor, Quantification

Send correspondence to: Thomas Rodt, Dept. of Radiology, Hannover Medical School, Carl-Neuberg-Str. 1, 30625 Hannover, Germany, Tel: 49-0511-532-3406, Fax: 49-0511-532-3797, E-mail: rodt.thomas@mh-hannover.de